Z. Phys. Chem. **224** (2010) 1119–1150 / **DOI** 10.1524/zpch.2010.6144

Heterogeneous Chemistry of Cl_2O and HOCl on Frozen Natural Sea Salt, Recrystallized Sea Salt, KCl and NaCl Solutions at 200 and 215 K

By Pascal Pratte and Michel J. Rossi*

Ecole Polytechnique Fédérale de Lausanne (EPFL), Laboratoire de Pollution Atmosphérique et sol (LPAS), Station 6, CH-1015 Lausanne, Switzerland

Dedicated to Prof. Dr. Reinhard Zellner on the occasion of his 65th birthday

(Received December 11, 2009; accepted March 21, 2010)

Heterogeneous Chemistry / Sea Salt / Cl_2O / HOCl

The HOCl heterogeneous reaction on frozen natural (NSS) and recrystallized (RSS) sea salt, KCl and NaCl solutions was studied using a low pressure flow reactor in order to measure the uptake coefficient γ and products of reaction. The HOCl sample used in these experiments always contained up to 25% Cl_2O which was also studied separately as a pure gas in order to understand the heterogeneous chemistry of both gases. By performing HOCl uptake on frozen NSS solution at 200 K and a gas-phase residence time of (1.6±0.6) s we obtained a steady state uptake coefficient $\gamma_{HOCl\ on\ NSS} = (2.5\pm0.7)\times10^{-3}$ and $\gamma_{Cl2O\ on\ NSS} = (2.8\pm0.8)\times10^{-3}$. On frozen KCl solution at 200 K we obtain $\gamma_{HOCl\ on\ KCl} = (2.8\pm1.3)\times10^{-3}$, identical to NSS, and $\gamma_{Cl2O\ on\ KCl} = (4.6\pm0.8)\times10^{-4}$. The main product formed during the uptake on frozen NSS solution is Cl_2 which is sustained for at least one hour. In contrast, only a transient Cl_2 flow (pulse) decreasing on the time scale of 100 s was observed on frozen KCl (NaCl) solution. 25±10 % of the HOCl taken up on all chloride-containing frozen substrates at 200 K react to produce Cl_2 at high HOCl concentration (4.5×10^{11} molecule cm^{-3}) and at a residence time of 1.6 s in comparison with twice that for Cl_2O. For smaller concentrations such as [HOCl] = 3.7×10^{10} molecule cm^{-3} and/or a shorter residence time (0.137±0.004s), HOCl uptake did not generate Cl_2 in contrast to Cl_2O. A single Br_2 burst event was monitored when a Cl_2O or HOCl/Cl_2O mixture is taken up on fresh frozen NSS solution during the first uptake at 200 K. Further Cl_2O or HOCl/Cl_2O uptake on the same sample, even after annealing at 240 K does not show an additional Br_2 pulse. This Br_2 release may be significant in the autocatalytic ozone destruction mechanism in the troposphere during polar sunrise. Some of the atmospheric implications of the present results are highlighted with emphasis on the preequilibrium $Cl_2O(ads) + H_2O(ice) \leftrightarrows 2\ HOCl(ads)$ between adsorbed HOCl and Cl_2O, with the latter being the gateway to reactive uptake of HOCl at low temperatures.

* Present address: Paul Scherrer Institut (PSI), Laboratorium für Atmosphärenchemie (LAC), OFLA008, CH-5232 Villigen PSI, Switzerland; E-mail: michel.rossi@epfl.ch.

1. Introduction

Essentially complete ozone loss is frequently observed in the boundary layer of the Arctic in the springtime [1]. Field measurements revealed that the ozone concentration decreases by approximately a factor of ten in a few hours [1] which seems to be correlated to a local maximum of [BrO] during sunrise [2–4]. This event has been called polar sunrise chemistry and has been associated with the presence of bromine containing species collected on filters. This suggests that bromine-containing species such as Br, HBr and HOBr play a leading role in the mechanisms of O_3 destruction. Moreover, there is experimental evidence from the field that chlorine atom concentrations are also elevated during these ozone-depletion periods owing to the observed chlorination of naturally occurring hydrocarbons that is consistent with the presence of an important marine halogen source [5]. Recent experimental results have confirmed the presence of Br and Cl precursor concentrations on the tens to hundreds of ppt level such as Br_2 [6,7], BrCl [6], HOBr, Cl_2 and HOCl [7]. Therefore, the search for an explanation of the underpinning chemical mechanism has focussed on catalytic cycles of Br which is well known from studies of global and polar stratospheric ozone depletion and is displayed in reactions (1) to (3):

$$Br_2 + h\nu \rightarrow 2Br \tag{1}$$

$$Br + O_3 \rightarrow BrO + O_2 \tag{2}$$

$$2\,BrO \rightarrow Br_2 + O_2 \tag{3}$$

Owing to the extremely short time scale of ozone destruction in polar sunrise chemistry the search for a mechanism has focussed on autocatalytic processes that include a degenerate chain branching step and are similar to combustion or explosion of hydrocarbon fuels, hence the alternative term “bromine explosion” for the description of polar sunrise chemistry. An autocatalytic process is one where one or more of the resulting reaction products are catalysts for the reaction under study in contrast to a case where a catalyst is added externally. A number of possible chemical reactions listed in reactions (4) to (7) including photochemistry involving aqueous sea salt (marine aerosol) [8,9] or frozen sea salt solution [10] have been proposed in order to explain the extremely short time scale of ozone loss, the chlorination of hydrocarbons and the postulated high halogen free radical concentration in the polar region which can attain values of up to 10^5 $Cl^{\bullet}$ cm^{-3} [11,12].

$$HOBr + Cl^- \rightarrow BrCl + OH^- \tag{4}$$

$$HOBr + Br^- \rightarrow Br_2 + OH^- \tag{5}$$

$$HOCl + Br^- \rightarrow BrCl + OH^- \tag{6}$$

$$BrCl + h\nu \rightarrow Br^{\bullet} + Cl^{\bullet} \quad (7)$$

During polar sunrise, a significant part of Br_2, Cl_2 and BrCl may be generated by heterogeneous chemistry of HOCl and HOBr which are mainly formed from the homogeneous gas phase reaction of OH and XO (X = Cl, Br) radicals, reaction (8):

$$HO_2^{\bullet} + XO^{\bullet} \rightarrow HOX + O_2 \quad (8)$$

The formation of HOX (X = Cl, Br) compounds contributes therefore towards a temporary reservoir of halogen compounds activated by their heterogeneous reactions on sea salt aerosol and/or frozen sea salt according to reactions (4) and (5) [11–13].

The autocatalytic nature stems from the fact that one Br atom, once reacted to HOBr following reaction (8), is able to volatilise marine bromide from sea spray aerosols or from frozen sea salt following reaction (5) and thereby form two potentially active Br atoms after photolysis of the precursor Br_2. It is the catalyst and needs to be present in only minute concentrations. This amounts to degenerate chain branching afforded by a heterogeneous reaction and continues until the BrO concentration is sufficiently high such that the catalytic cycle (reactions (1) to (3)) will take over. The rate determining step of the autocatalytic mechanism is the formation of HOBr in reaction (8) and is superseded by reaction (3) once the reaction has switched from autocatalytic to catalytic. The mechanistic investigations have mainly focussed on the role of Br rather than Cl because of faster heterogeneous reaction rates of HOBr [14]. In addition, there are potential complications with HOCl because it is unstable with respect to its anhydride Cl_2O which is also reactive with marine halides X^- as shown below.

Sea salt deposited on the polar snow pack may contribute to the conversion of halogen reservoir molecules to reactive species by heterogeneous processes that deplete the ice/salt surface. This process competes with similar heterogeneous reactions that involve deliquescent sea salt aerosols. Only when the heterogeneous reactions (4) and (5) of HOBr on ice and snow are included does the simulation of tropospheric ozone destruction agree with field measurements through halogen activation [15]. However, only few data are available for HOCl heterogeneous reactions on marine aerosol and sea ice in comparison to uptake experiments of HOBr or HOCl performed on solid substrates [16–20].

It was suggested that HOCl could be an important temporary reservoir for chlorine in the marine boundary layer because it reacts very slowly with ozone ($k^{II} < 4.0 \times 10^{-16}$ cm^3 molecule^{-1} s^{-1}) [21] and does not react with hydrocarbons. Despite the fact that HOCl has never been measured in the dark winter season in the polar boundary layer, it may in principle be formed by radical recombination (8) [22]. The absorption coefficient of HOCl is given in the literature [23,24] within the critical 300–380 nm wavelength region and leads to a photolysis lifetime of less than one hour using the measured photodissociation rate constant at the surface of the earth. This short lifetime suggests that HOCl

is an ineffective chlorine reservoir under solar radiation but in turn could be effective in the arctic region during the winter season in the absence of actinic radiation.

Huff and Abbatt performed uptake experiments of HOCl(g) in a laminar low pressure flow reactor in which the walls were coated with a frozen NaCl solution at 233 K [25]. They used [HOCl] = 3×10^{12} cm^{-3} at a total pressure of He between 1 and 2 Torr and concluded that HOCl is unreactive on frozen sea salt. We took this work as a starting point of the present contribution towards the knowledge of heterogeneous reactions of HOCl which has not been as thoroughly investigated as HOBr owing to the fact that the role of HOCl in polar sunrise chemistry is less clear than for HOBr. In addition, the equilibrium between HOCl and Cl_2O, the latter of which is currently of no atmospheric interest, and the anticipated reactivity of both components on liquid and frozen halide solutions make this a chemical system that we wished to investigate further. The observational evidence for HOCl is fairly weak for the troposphere, however, it has been unambiguously identified in the middle and lower stratosphere in satellite IR and FIR spectrometry [26]. Recently, the rate constant of reaction (8) has come under debate in the interest of obtaining a satisfactory fit to HOCl profiles obtained by satellite measurements [26].

We present here kinetic results of HOCl uptake mainly on frozen KCl and natural sea salt (NSS) solutions at 200 and 215 K that are in the range of relevant temperatures during the polar winter in the MBL. In addition, the products of reaction released into the gas-phase were monitored in order to quantify the rate at which gas-phase HOCl is converted to Cl_2, the precursor for chlorination of naturally occurring hydrocarbons. We also focussed on differences between HOCl uptake coefficients measured on frozen KCl, recrystallised sea salt (RSS) and natural sea salt (NSS) solutions as well as products formed. In addition, we tested the role of acidity for the formation of products both on NSS and KCl frozen solution.

2. Experimental setup

Experiments were performed in a Teflon-coated low pressure flow reactor that is suited for the measurement of heterogeneous process. A detailed description of this technique has been given elsewhere [28]. Briefly, the Knudsen flow reactor is mounted on a differentially pumped high vacuum chamber equipped with a cryogenic and a turbomolecular pump. A given number of molecules are injected into the reactor by a glass capillary inlet before effusing out of the escape orifice after a lifetime τ ($1/k_{esc}$ (s^{-1}) with k_{esc} being the measured escape rate constant $/s^{-1}$) to form a modulated (thermal) molecular beam by a rotating chopper located in the upper chamber. The quadrupole mass spectrometer signal is then processed by a digital lock-in amplifier in order to separate the contribution of the molecular beam from the background gas phase.

Table 1. Escape rate constants k_{esc} of HOCl, Cl_2 and Cl_2O measured at 300 K and typical gas concentrations [G] for the 4 and the 14 mm diameter escape aperture.

	k_{esc} ($\pm 0.2\ s^{-1}$) / [G]$\times 10^{11}$ molecule cm^{-3}		
Escape aperture (mm)	HOCl	Cl_2	Cl_2O
4	0.6 / 4.5	0.5 /	0.4 / 2.7
14	7.3 / 0.37	6.3 /	5.7 / 0.19

In order to measure the uptake coefficient $\gamma(HOCl,Cl_2O)$ on the frozen substrates we quantitatively measured the HOCl and the Cl_2O molecules that have been taken up as a function of time. To this end, steady state experiments were performed in the low pressure flow reactor using concentrations ranging from 10^{10} to 10^{12} molecule cm^{-3}. An initial flow rate F_{in} (molecule s^{-1}) is admitted into the reactor and after a short transition time, the effusive flow rate F_{out} equals the incoming flow rate F_{in} if no chemical loss is admitted, that is when the sample compartment is isolated from the inflow. The residence time τ and the gas concentration may be varied by changing either the flow or the size of the escape orifice. When the sample compartment is open to the flow, part of the gas is lost on the substrate resulting in a competition between the escape rate ($k_{esc}N$, with N being the total number of gas molecules in the reactor) and the rate of loss ($k_{loss}N$). At steady state we obtain the following balance:

$$\frac{dN}{dt} = F_{in} - Nk_{esc} - Nk_{loss} = 0 \tag{9}$$

Rearrangement of equation (9) leads to equation (10) which relates the ratio F_{in}/F_{out} to the escape rate constant k_{esc} and results in the heterogeneous loss rate constant k_{loss}:

$$k_{loss} = \left(\frac{F_{in}}{F_{out}} - 1\right)k_{esc} \tag{10}$$

Commonly, we used a normalised form of k_{loss}, namely the uptake coefficient γ that expresses the probability that a molecule colliding with a surface is captured. We defined γ simply by the first order loss rate constant k_{loss} divided by the frequency of collision ω in s^{-1}. In addition, k_{esc} was measured by monitoring the exponential decay rate of the MS signal by halting F_{in} in the absence of substrate. The escape rates k_{esc} were measured for the different escape apertures, namely for the 4 and 14 mm diameter orifices (Table 1). The concentration of a gas G was calculated by using the initial flow rate F_{in} and the measured k_{esc} using the expression $[G] = F_{in}/Vk_{esc}$ with values summarized in Table 1. HOCl, Cl_2O, Cl_2 and Br_2 were monitored at m/e 52, 51, 70 and 160, respectively.

2.1 Sample preparation

Three types of salt samples were used, namely KCl (NaCl) (Fluka, purity > 99.5%), recrystallized sea salt RSS (Hawaiian Salt, Honolulu, PA AKAI INC.)

and NSS (sel de Guérande, DIEPAL-NSA) which is a natural non-processed sea salt obtained by pan evaporation (open air). Solutions of KCl (NaCl), NSS and RSS were made from the dissolution of salts in bidistilled water (35g/L) and subsequent filtration in order to mimic the salt concentration of sea water [29]. The salt solutions were degassed in a vacuum line by performing two freeze-pump-thaw cycles before pouring the salt solution, typically 5 ml, into the gold coated copper cryogenic support that is described elsewhere [30]. Subsequently, the temperature of the salt solution was decreased at a rate of 0.2 K s^{-1} down to 200 or 215 K in order to produce frozen sea salt [27]. All frozen solutions were cooled down following the same procedure. In fact, different ice preparation methods led to different uptake kinetics in the past [31]. It is known that the cooling rate affects the halide distribution in the bulk and on the surface of ice [32]. If the freezing rate is slow bulk ice will concentrate most of the salt on the substrate surface by segregation processes. However, in an atmospheric context sea water freezes too quickly to allow segregation of halide from the bulk. In some cases, KCl (NaCl) solutions were acidified using a commercial buffered solution containing 0.068 M NaOH, 0.056 M citric acid and 0.044 M NaCl to buffer the frozen salt solution at pH = 4 in order to study the effect of acidity on the rate of Cl_2 formation.

2.2 HOCl and Cl_2O synthesis

Cl_2 was admitted to a vessel containing HgO powder (Fluka, puriss > 99.0%) held at 77 K which was kept for 24 hours at 190 K to allow the following reaction to occur:

$$HgO(s)+2Cl_2(g)\rightarrow Cl_2O(g)+HgCl_2(s) \tag{11}$$

Cl_2O, absorbing at $\lambda < 700$ nm, was transferred to a trap containing approximately 2 ml of frozen bidistilled water at 77 K that was subsequently warmed in a water bath to ambient temperature. The cherry-colored Cl_2O liquid reacts with liquid water to produce HOCl(l) upon Cl_2O hydrolysis according to reaction (12).

$$Cl_2O(l) + H_2O(l) \leftrightarrows 2\ HOCl(l) \tag{12}$$

The HOCl sample was kept at 190 K as a stock solution for further use.

2.3 Calibration procedure

Because HOCl is in equilibrium (12) with Cl_2O, increasing concentrations of HOCl will shift the equilibrium towards Cl_2O under static conditions. In order to limit the formation of Cl_2O, we pumped on the sample in order to lower the total pressure. Even under those non-equilibrium conditions 25±10 % of Cl_2O remained in the HOCl sample. At these experimental conditions the flow rate measurement of HOCl into the flow reactor (F_{in}(HOCl)) could not be performed

by observing the pressure drop in the calibrated volume because the pressure in the vacuum line is under 50 mTorr which is too small for a reliable pressure measurement using an absolute Baratron gauge (MKS Baratron 122AA-00010AB). In order to calibrate the MS signal for HOCl, a titration was performed on a vapor-deposited ice substrate. In contrast, the impurity Cl_2O has been calibrated in the usual way by measuring its pressure drop in a calibrated volume as described in the literature [31]. In order to enable the titration of HOCl, Bulk (B) ice was prepared at 200 K in the cryogenic support device [30]. Subsequently, we deposited an amount of HCl on B ice in excess over HOCl before isolating the sample by sealing off the sample compartment. The HOCl source was held at 197±1 K under differential pumping conditions by using a roughing pump protected by a cold trap. A steady-state flow of HOCl was established into the flow reactor and was allowed to react with the HCl/ice sample. The gas phase HOCl and the Cl_2O impurity are titrated by excess adsorbed HCl following reactions (13) and (14):

$$Cl_2O(g) + HCl(ads) \rightarrow Cl_2(g) + HOCl(ads) \quad (13)$$

$$HOCl(g) + HCl(ads) \rightarrow H_2O(ads) + Cl_2(g) \quad (14)$$

$$Cl_2O(g) + 2HCl(ads) \rightarrow 2Cl_2(g) + H_2O(ads)$$

The same titration procedure was performed for pure Cl_2O. This leads to the conclusion that for each Cl_2O taken up, two Cl_2 were released to the gas phase. In addition, we believe that HOCl(ads) generated in reaction (13) is converted to $Cl_2(g)$ in reaction (14). By using these reactions for the titration of the HOCl/Cl_2O mixture, the calibration constant for HOCl is given by equation (15).

$$K_{cal}^{(HOCl)} = \frac{K_{cal}^{(Cl_2)} I^{(Cl_2)} - 2K_{cal}^{(Cl_2O)} I^{(Cl_2O)}}{I^{(HOCl)}} \quad (15)$$

where $I^{(X)}$ and $K_{cal}^{(X)}$ are the measured MS signal and the calibration constant for the molecule X (X = Cl_2, Cl_2O, HOCl), respectively. The absolute calibration for the Cl_2 mass signal was obtained from authentic samples of pure Cl_2.

3. Results and discussion on Cl_2O and HOCl uptake

3.1 Uptake kinetics of HOCl and pure Cl_2O on bulk ice at 200 K

The HOCl sample used in the present work inevitably contains up to 25% Cl_2O following equation (12). It is likely that the Cl_2O "impurity" in HOCl does not correspond to the equilibrium fraction because the mixture was not let to equilibration under the used experimental conditions. Consequently, we need to take into account the presence of Cl_2O by performing uptake experiments of pure Cl_2O on all studied substrates as a reference in order to provide a comparison for

the uptake experiment of the $HOCl/Cl_2O$ mixture. Before performing uptake experiments on the frozen salt solution, we have studied the uptake of pure Cl_2O and the $HOCl/Cl_2O$ mixture on bulk (B) ice from frozen liquid water [31].

The uptake coefficient γ for the $HOCl/Cl_2O$ mixture on bulk ice is $\gamma_{ss}(HOCl) = (5.5\pm0.4)\times10^{-4}$ and $\gamma_{ss}(Cl_2O) = (5.3\pm0.6)\times10^{-4}$, respectively. For uptake of pure Cl_2O, we obtain $\gamma_{ss}(Cl_2O) = (2.8\pm0.7)\times10^{-4}$, lower by a factor of two compared to the mixture. These results directly follow from displays in Figures 9 and 10 (see Appendix). These uptake experiments show that γ_{ss} for each component of the $HOCl/Cl_2O$ mixture is similar while pure Cl_2O uptake results in a γ_{ss} value smaller by a factor of two compared to the simultaneous measurement of $\gamma_{ss}(Cl_2O)$ and $\gamma_{ss}(HOCl)$. It seems that Cl_2O uptake on pure B ice is accelerated by HOCl, perhaps by hydrogen bonding owing to the presence of adsorbed HOCl.

In addition, we note (Figure 9) that no product was formed for the $HOCl/Cl_2O$ mixture at 200 K. Conversely, in the case of pure Cl_2O uptake, slow HOCl formation and Cl_2O decomposition to Cl_2 occurred (Figure 10) as displayed in equations (16) and (17):

$$Cl_2O \rightarrow Cl_2 + \tfrac{1}{2}\,O_2 \qquad \text{(heterogeneous decomposition)} \tag{16}$$

$$H_2O + Cl_2O \rightarrow 2HOCl \qquad \text{(heterogeneous hydrolysis)} \tag{17}$$

This shows that HOCl and Cl_2O are not rapidly converted to Cl_2 on pure B ice at 200 K. These reference experiments performed on Bulk (B) ice enable the comparison of the conversion efficiency of HOCl and Cl_2O to Cl_2 on frozen salt solutions performed under the same conditions. The chosen HOCl and Cl_2O concentrations are high in order to enable observation of the possible formation of Cl_2, namely 4.5×10^{11} and 1.5×10^{11} molecule cm^{-3}, respectively. In the absence of any major product formation we conclude that the uptake of both HOCl and Cl_2O is non-reactive and leads to adsorption of both gases on the surface of ice. Without investigation of the condensed phase we are unable to state on the possible inverse of reaction (12) upon HOCl adsorption.

3.2 Pure Cl_2O uptake on frozen KCl and NSS solution at $[Cl_2O] > 10^{11}$ molecule cm^{-3}

Figure 1a (upper left panel) displays a Cl_2O uptake experiment on frozen KCl solution as a function of time using $[Cl_2O] = 2.3\times10^{11}$ molecule cm^{-3} corresponding to $F_{in}(Cl_2O) = 1.7\times10^{14}$ molecule s^{-1}. This is similar to the concentration of the Cl_2O impurity found in the used $HOCl/Cl_2O$ mixture. When the frozen KCl solution is exposed to Cl_2O at t = 80 s, a transient production of Cl_2 is observed that is accompanied by a continuous production of HOCl reaching a steady state level at t = 400 s. In contrast, the Cl_2 production is decreasing to a

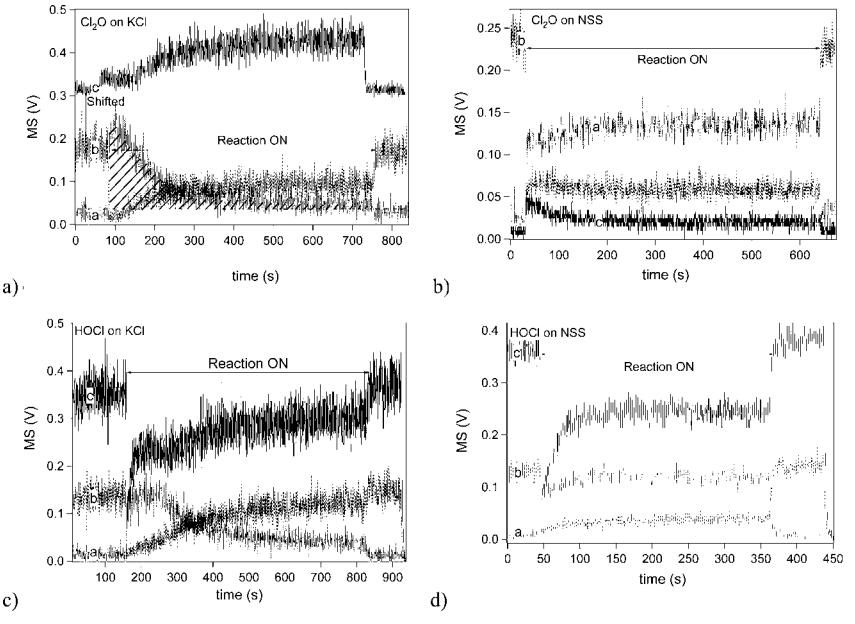

Fig. 1. a) and b) represent Cl_2O uptake performed on frozen KCl and NSS solution, respectively, at 200 K and using the 4 mm diameter escape aperture. c) and d) represent HOCl uptakes performed on frozen KCl and NSS solution, respectively. The dotted line (trace a) represents Cl_2, the hashed curve is Cl_2O (trace b) and the solid curve is the HOCl (trace c) MS signal. In a) $F_{Cl2O} = (1.7\pm0.4)\times10^{14}$, in c) $F_{HOCl} = 7.6\times10^{14}$ and $F_{Cl2O} = 1.9\times10^{14}$ molecule s^{-1}. In b) $F_{Cl2O} = (1.9\pm0.5)\times10^{14}$ and in d) $F_{HOCl} = (9.0\pm0.3)\times10^{14}$ and $F_{Cl2O} = (2.1\pm0.5)\times10^{14}$ molecule s^{-1}.

low steady state level after the primary burst, presumably because of the accumulation of OH on the surface according to reactions (12), (18) and (19):

$$Cl_2O(g) + H_2O(ads) \leftrightarrows 2\ HOCl(ads) \tag{12}$$

$$HOCl(ads)+Cl^- + M^+ \rightarrow Cl_2(g)+M^+ + OH^- \ (M^+ = Na^+, K^+, Ca^{++}, \ldots) \tag{18}$$

$$Cl_2O(g) + Cl^- \rightarrow ClO^- + Cl_2(g) \tag{19}$$

Uptake experiments of pure Cl_2O were also performed on frozen NSS solution at 200 K for which a typical uptake is shown in Figure 1Ib for $[Cl_2O]$ given in Table 1. At t = 30 s, the plunger is lifted and the substrate exposed to Cl_2O which leads to steady state formation of Cl_2 accompanied by slow formation of HOCl. This steady state formation of Cl_2 displayed in Figure 1b is in contrast to the corresponding uptake of Cl_2O performed on KCl frozen solution (Figure 1a). Cl_2O uptake was also performed on frozen NaCl and RSS solution which show identical behaviour in terms of kinetics and formation of products to frozen KCl

solution. This is in contrast to uptake of Cl_2O on NSS that is characterized by sustained formation of Cl_2 and slow formation of HOCl. The major difference between NSS and RSS frozen solution is that NSS contains fatty acids, polyfunctional partially oxidized organics or humic acid-like substances (HULIS) [33] that may affect the formation of Cl_2. We believe that NSS is sufficiently internally buffered to be able to neutralize the resulting hydroxyl ion in reaction (18) so as to support a sustainable formation of Cl_2. In contrast, the formation of Cl_2 comes to a halt in unbuffered frozen solutions such as KCl and RSS because the halide displacement resulting in Cl_2 is a general acid catalyzed reaction requiring the presence of HOCl rather than ClO^-. Alternatively, NSS may contain organic matter that is easily oxidized by either HOCl or Cl_2O thereby reducing the chlorine to Cl_2.

3.3 Mass balance for pure Cl_2O uptake

After each uptake experiment, the substrate is isolated from the reactive gas in order to halt the reaction and measure the flow rate. The area of the MS signal corresponding to the reactant lost or product formed was evaluated and leads to the number of molecules taken up or produced during the reaction. As an example, the dashed area in Figure 1a corresponds to the yield of Cl_2 on the time scale of the experiment. After the experiment, the surface was annealed at 240 K in order to measure desorbed products at 240 K.

The mass balance from Figure 1a between Cl_2O uptake on frozen KCl solution and product formation may be expressed as follows: 7.3×10^{16} Cl_2O molecules were taken up against production of 8.4×10^{16} HOCl and 4.9×10^{16} Cl_2 molecules produced (see Table 5). After uptake, the frozen solution was annealed at 240 K resulting in the desorption of 1.6×10^{15} Cl_2O corresponding to approximately 2% of the total Cl_2O initially taken up. However, an important fraction of adsorbed HOCl is collected during thermal desorption corresponding to 2×10^{16} molecules. During thermal desorption, no Cl_2 was measured even if the plunger was lowered for 20 minutes in order to let the frozen film react. Consequently, no delayed Cl_2 production is observed in the isolated sample compartment.

The mass balance expressed per chlorine atom is established including the products of desorption listed in Table 5 for Cl_2O uptake according to equation (20) where the brackets correspond to molar yields:

$$2\times(Cl_2O_{\text{taken up}}) = HOCl_{\text{produced}} + HOCl_{\text{desorbed}} + 2\times(Cl_2O_{\text{desorbed}}) + (Cl_2)_{\text{produced}} \quad (20)$$

In equation (20), we assume that for each Cl_2 produced, one $Cl^\bullet$ came from the Cl_2O source while the second $Cl^\bullet$ was contributed as halide from the salt substrate surface.

The chlorine mass balance displayed in Table 5 between Cl dosed and recovered is excellent, namely 1.46×10^{17} Cl dosed vs. 1.56×10^{17} Cl recovered. This

means that all chlorine deposited is recovered from the KCl frozen solution held at 200 K for initial $[Cl_2O] > 1\times10^{11}$ molecule cm^{-3}. The data taken from Figure 1a and Table 5 reveal that 4.9×10^{16} Cl_2 were produced which means that 4.9×10^{16} surface (or near-surface) chloride ions were consumed. The ratio of the surface Cl^- to the total chlorine taken up is $4.9\times10^{16}/2\times0.73\times10^{17}$ = 0.33±005 which means that 33% of the deposited Cl from Cl_2O react with Cl^- at the substrate interface on frozen KCl solution at 200 K for $[Cl_2O] > 10^{11}$ molecule cm^{-3} (see Table 5, next to last column).

The same mass balance check was performed for pure Cl_2O uptake at 200 K on NSS frozen solution and again leads to excellent agreement between deposited and recovered chlorine as displayed in Table 5 as well. As an example, data on Cl_2O uptake on NSS frozen solution at 200 K for $[Cl_2O] > 10^{11}$ molecule cm^{-3}, displayed in Figure 1b are summarized in Table 5. In Figure 1b, 1.41×10^{17} Cl_2O were taken up whereas 0.97×10^{16} HOCl and 1.96×10^{17} Cl_2 were generated. Thermal desorption led to 3.7×10^{15} Cl_2O and 7×10^{16} HOCl. Using equation (20) we obtain excellent agreement between dosed and recovered chlorine (2.82×10^{17} vs. 2.83×10^{17} molecule). The ratio of the unreacted to dosed Cl_2O is approximately 2.5%, and approximately 70±7 % of the deposited chlorine reacts with surface Cl^-. We note an important relative increase in surface reactivity of Cl^- to Cl_2 in going from frozen KCl to NSS solution at 200 K for $[Cl_2O] > 10^{11}$ molecule cm^{-3}.

The yield of Cl_2 on frozen KCl and NSS solution was plotted in Figure 2 as a function of Cl_2O taken up for several experiments. Figure 2 shows that the yield of Cl_2 per Cl_2O taken up is larger on frozen NSS than on KCl solution at 200 K. As an example, 1×10^{17} Cl_2 have been produced on NSS compared to 0.3×10^{17} on KCl, NaCl and RSS frozen solution for 1×10^{17} Cl_2O taken up. This difference in slope is consistent with the fast rate of formation of Cl_2 and the slow rate of formation of HOCl as displayed in Figure 1b. It results in a slope of 1.11±0.30 displayed in Figure 2. In contrast, the experiment displayed in Figure 1a shows a slow rate of formation of Cl_2 and a fast rate of formation of HOCl resulting in a slope of 0.40±0.11 in Figure 2, a factor of 2.8 lower than NSS. Apparently, the rates of formation of Cl_2 by surface halogen exchange with chloride and formation of HOCl by hydrolysis are competing against each other in Cl_2O uptake at 200 K. The predominant formation of Cl_2 from pure Cl_2O on frozen NSS may be either explained by oxidation of organic matter and concomitant reduction of Cl_2O or by predominant reverse disproportionation (or halogen exchange). Hydrolysis of Cl_2O resulting in HOCl is apparently not competitive and therefore represents the minority channel on NSS. In contrast, on frozen KCl salt solutions the competitive situation is reversed with the hydrolysis channel

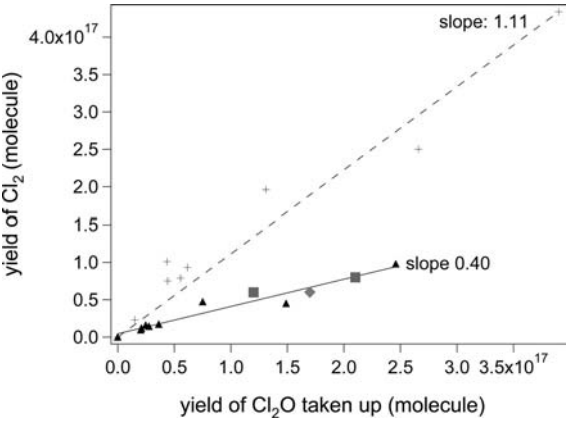

Fig. 2. Correlation between the yield of Cl_2 and Cl_2O taken up. Uptake experiment of pure Cl_2O on frozen KCl (▲), NSS (+), NaCl (◆) and recrystallized RSS (■) solution at 200 K for $[Cl_2O] = 2.7\times10^{11}$ molecule cm^{-3}. Each point corresponds to a separate experiment and the integration time is 700±50 s.

being dominant and the oxidation/reduction channel being outrun by hydrolysis, perhaps owing to the absence of organic matter in the KCl salt solution.

3.4 Uptake of the HOCl/Cl_2O mixture on frozen KCl and NSS solution

The uptake of the HOCl/Cl_2O mixture on frozen KCl and NSS solution has been measured relative to pure Cl_2O uptake. Figure 1c shows a typical uptake experiment of a HOCl/Cl_2O mixture on frozen KCl solution as a function of time at 200 K for [HOCl] > 10^{11} molecule cm^{-3}. At t = 160 s, the plunger is lifted and a constant rate of formation of Cl_2 is observed to 250 s, after which the Cl_2 rate of formation decreases. In contrast, the uptake of a HOCl/Cl_2O mixture on frozen NSS solution reveals a continuous formation of Cl_2 upon lifting the plunger at t = 50 s (Figure 1d). The formation of Cl_2 remains constant during more than one hour (data not shown). Repetitive uptake experiments of HOCl/Cl_2O mixtures on fresh and poisoned frozen KCl solutions are displayed in Figures 11a and 11b, respectively. It appears that the Cl_2 yield is smaller for frozen KCl solution that has already been exposed to the HOCl/Cl_2O mixture compared to the fresh substrate. Furthermore, the Cl_2O uptake (Figure 11a and 11b, trace (b)) saturates at 250 s for a poisoned substrate whereas it saturates after 400 s on a fresh frozen KCl solution. Despite the saturation of the Cl_2O uptake Cl_2 formation is still on-going at $F(Cl_2) = 3\times10^{13}$ molecule s^{-1}. The only possible source for the production of Cl_2 is therefore HOCl uptake from the HOCl/Cl_2O mixture at a flow rate of 1×10^{14} molecule s^{-1}. On a relative basis, for ten HOCl taken up, three are converted to Cl_2 while seven stay adsorbed on the substrate and will be recovered during thermal desorption at 240 K in mass balance experiments.

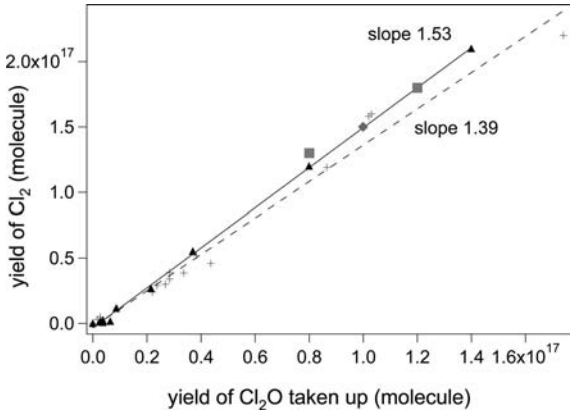

Fig. 3. Correlation between the yield of Cl_2 and Cl_2O taken up. Uptake experiment of the $HOCl/Cl_2O$ mixture on frozen KCl solution (▲), NSS (+), NaCl (◆) and recrystallized sea salt (■) at 200 K for [HOCl] = 4.5×10^{11} molecule cm^{-3}. Each point corresponds to a separate experiment and the integration time is 700±50 s.

Role of acidity on frozen KCl solution

In order to find out how acidity could affect the yield of Cl_2 formation, we have performed uptakes of $HOCl/Cl_2O$ mixtures on buffered frozen KCl solutions at 200 K and pH = 4 for [HOCl] > 10^{11} molecule cm^{-3} as displayed in Figure 12. The formation of Cl_2 remains nearly constant during uptake of the $HOCl/Cl_2O$ mixture on the buffered frozen KCl solution akin to neutral frozen NSS solution as shown in Figure 1d. In fact, the buffered solid allows the neutralisation of OH^- produced in reaction (18). Buffering is obviously not necessary for sustaining Cl_2 formation on frozen NSS solutions, presumably owing to their natural buffering capacity. As long as acidity is available to neutralize OH^- (reaction (18)), it prevents the neutralization of HOCl that would accumulate non-reactive hypochlorite salts on the frozen KCl surface and thereby poison the surface with respect to further reaction of both HOCl and Cl_2O.

Mass balance for the uptake of the $HOCl/Cl_2O$ mixture on frozen KCl and NSS solution

The mass balance was also checked for the uptake of the $HOCl/Cl_2O$ mixture on frozen KCl and NSS solution using equation (21):

$$2\times(Cl_2O_{taken\ up}) + (HOCl_{taken\ up}) = (HOCl_{desorbed}) + 2\times(Cl_2O_{desorbed}) + (Cl_2)_{produced} \quad (21)$$

Taken as an example from Table 5, total chlorine taken up (1.17×10^{17} molecule) equals the recovered amount (1.14×10^{17} molecule) for a frozen KCl solu-

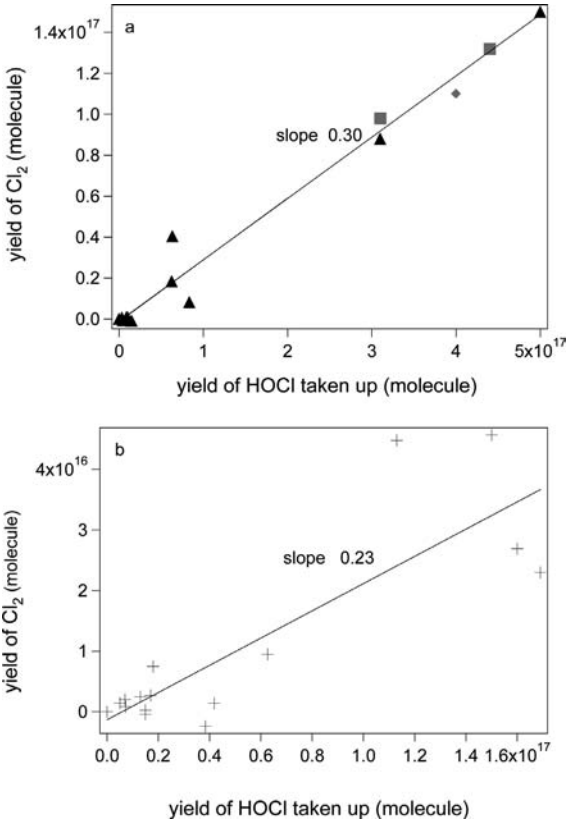

Fig. 4. The fractional yield of Cl_2 generated from HOCl reacting at 200 K plotted as a function of the HOCl taken up on frozen KCl (▲), NaCl (◆) and on recrystallized SS (■) after correction for Cl_2 production owing to Cl_2O uptake following equation (22), (a). Similar experiments were performed on frozen NSS solution for [HOCl] = 4.5×10^{11} molecule cm^{-3}, (b). Each point represents a new sample at different reaction times and at identical [HOCl]; the integration time is 700±50 s.

tion. The ratio between the surface Cl^- estimated from the measured Cl_2 and the total chlorine deposited yields 0.50±0.06 which is larger by 50% (0.50/0.33) compared to the value measured for pure Cl_2O interacting with frozen KCl solution, in agreement with Table 5.

The presence of HOCl apparently leads to an additional depletion of surface Cl^-. Consequently, the HOCl taken up could contribute to the formation of 50% more Cl_2 with respect to uptake of Cl_2O alone if we assume that Cl_2O and HOCl are both taken up *independently*. As will be pointed out below, this assumption may not be valid in the present case. Results displayed in Tables 2 to 4 reveal that the uptake kinetics of Cl_2O is somewhat inhibited by the presence of HOCl

Table 2. Summary of γ values for fresh, that is non-poisoned, frozen salt solution at 200 K using the 4 and 14 mm diameter escape aperture.

Fresh frozen salt solution		KCl		NSS	
	Formation of HOCl	Slow for pure Cl_2O uptake		None for pure Cl_2O uptake	
	Formation of Cl_2	Transient for HOCl uptake and for pure Cl_2O uptake		Fast for HOCl and pure Cl_2O uptake	
Kinetics (γ)	φ(mm)	4	14	4	14
HOCl/Cl_2O mixture	HOCl $(Cl_2O)_0$	$(1.2\pm0.5)\times10^{-2}$	$(8.3\pm2.5)\times10^{-2}$	$(1.6\pm0.5)\times10^{-2}$	$(5.4\pm1.6)\times10^{-2}$
	HOCl $(Cl_2O)_{SS}$	$(2.8\pm1.3)\times10^{-3}$	$(2.5\pm0.7)\times10^{-2}$	$(2.5\pm0.7)\times10^{-3}$	$(2.6\pm0.8)\times10^{-2}$
	$(Cl_2O)_0$	$(3.0\pm1.1)\times10^{-2}$	$(1.8\pm0.6)\times10^{-1}$	$(1.6\pm0.6)\times10^{-2}$	$(1.8\pm0.4)\times10^{-1}$
	$(Cl_2O)_{SS}$	$(4.6\pm0.8)\times10^{-4}$	$(1.1\pm0.3)\times10^{-1}$	$(1.8\pm0.9)\times10^{-2}$	$(1.6\pm0.6)\times10^{-1}$
Pure Cl_2O	$(Cl_2O)_0$	$(4.5\pm1.4)\times10^{-2}$	$(2.8\pm1.1)\times10^{-1}$	$(3.3\pm1.4)\times10^{-2}$	$(2.5\pm0.7)\times10^{-1}$
	$(Cl_2O)_{SS}$	$(4.7\pm1.2)\times10^{-3}$	$(1.4\pm0.5)\times10^{-1}$	$(2.8\pm0.8)\times10^{-3}$	$(2.3\pm0.6)\times10^{-1}$

Table 3. Summary of γ values for a poisoned (contaminated) frozen salt solution at 200 K using the 4 and 14 mm diameter escape aperture.

Contaminated frozen salt solution		KCl		NSS	
	Formation of HOCl	Slow for pure Cl_2O uptake		None for pure Cl_2O uptake	
	Formation of Cl_2	Transient for HOCl uptake and for pure Cl_2O uptake		Fast for HOCl and pure Cl_2O uptake	
Kinetics (γ)	φ(mm)	4	14	4	14
HOCl/Cl_2O mixture	HOCl $(Cl_2O)_0$	$(5.2\pm2.3)\times10^{-2}$	$(3.6\pm0.5)\times10^{-1}$	$(8.2\pm2.2)\times10^{-3}$	$(1.1\pm0.6)\times10^{-1}$
	HOCl $(Cl_2O)_{SS}$	$(3.7\pm1.3)\times10^{-3}$	$(1.7\pm0.7)\times10^{-2}$	$(1.3\pm0.7)\times10^{-3}$	$(2.0\pm0.8)\times10^{-2}$
	$(Cl_2O)_0$	$(2.1\pm0.9)\times10^{-2}$	$(2.7\pm1.6)\times10^{-1}$	$(2.8\pm1.0)\times10^{-2}$	$(2.3\pm0.4)\times10^{-1}$
	$(Cl_2O)_{SS}$	0	$(4.8\pm1.9)\times10^{-2}$	$(1.2\pm1.2)\times10^{-2}$	$(1.0\pm0.3)\times10^{-1}$
Pure Cl_2O	$(Cl_2O)_0$	$(5.1\pm1.4)\times10^{-2}$	$(2.8\pm0.9)\times10^{-1}$	$(3.4\pm1.4)\times10^{-2}$	$(2.4\pm0.9)\times10^{-1}$
	$(Cl_2O)_{SS}$	$(1.9\pm0.7)\times10^{-3}$	$(8.0\pm2.1)\times10^{-2}$	$(6.7\pm0.8)\times10^{-3}$	$(2.4\pm1.1)\times10^{-1}$

which suggests a lower reactivity of HOCl on both frozen KCl as well as NSS solution compared to Cl_2O.

For the frozen NSS solution we found that 20% of the produced Cl_2 originates from HOCl (0.85/0.70 = 1.21, see Table 5). This seemingly lower enhancement of Cl_2 production owing to the presence of HOCl for frozen NSS compared to KCl solution stems from the fact that the uptake of pure Cl_2O on frozen NSS is already so important that it leaves no room for a large additional effect due to HOCl adsorption because of surface saturation of the uptake. In order to illustrate the yield difference of Cl_2 on frozen KCl and NSS solution upon uptake of the HOCl/Cl_2O mixture, we have plotted the yield of Cl_2 as a function of the Cl_2O taken up in Figure 3. We conclude that the Cl_2 yield is marginally larger on frozen KCl, NaCl or RSS solution compared to frozen NSS solution. When

Table 4. Summary of γ values for fresh frozen salt solutions at 215 K using the 4 mm diameter escape aperture.

Fresh Sample frozen solution		KCl	NSS
	Formation of HOCl	Slow for pure Cl_2O uptake	None for pure Cl_2O uptake
	Formation of Cl_2	Transient for HOCl uptake and for pure Cl_2O uptake	Fast for HOCl and pure Cl_2O uptake
Kinetics (γ) HOCl/Cl_2O mixture	HOCl $(Cl_2O)_0$	$(3.7\pm0.8)\times10^{-3}$	$(5.2\pm1.8)\times10^{-3}$
	HOCl $(Cl_2O)_{SS}$	$(2.1\pm0.6)\times10^{-3}$	$(4.6\pm1.4)\times10^{-3}$
	$(Cl_2O)_0$	$(3.0\pm0.9)\times10^{-2}$	$(3.0\pm1.1)\times10^{-2}$
	$(Cl_2O)_{SS}$	$(1.5\pm0.3)\times10^{-2}$	$(2.1\pm0.7)\times10^{-2}$
Pure Cl_2O	$(Cl_2O)_0$	$(4.2\pm1.1)\times10^{-2}$	$(4.5\pm1.2)\times10^{-2}$
	$(Cl_2O)_{SS}$	$(1.4\pm0.4)\times10^{-3}$	$(3.1\pm0.9)\times10^{-2}$

comparing Figures 2 and 3 the most striking feature is the differing slope for Cl_2 formation between uptake of pure Cl_2O (Figure 2) or a mixture of $Cl_2O/HOCl$ (Figure 3). Table 5 reveals that for pure Cl_2O uptake the Cl_2 yield increases by a factor of four in going from frozen KCl to NSS solution, whereas the yield of Cl_2O taken up only increases by a mere factor of two at a given initial concentration. In contrast, for the mixture $Cl_2O/HOCl$ both the Cl_2 as well as the quantity of Cl_2O taken up increase by a factor of four which leaves the slope in Figure 3 practically unchanged (1.53 vs. 1.39) when comparing frozen KCl with NSS solution. One should be aware that the enhancement factors from Table 5 refer to individual experiments whereas the slope changes in Figures 2 and 3 result from a least-squares fit to several experiments, thus corresponding to an average. This is the principal reason for the difference between the slope ratio of 2.8 displayed in Figure 2 compared to a factor of four difference in Cl_2 yield from Table 5 in going from KCl to NSS, both for pure Cl_2O and $HOCl/Cl_2O$.

Cl_2 formation from HOCl uptake

In order to quantify the amount of HOCl taken up which forms Cl_2 on frozen KCl solution, several $HOCl/Cl_2O$ uptakes were performed. Under the assumption that HOCl and Cl_2O interact independently on frozen solution (see remark above), the slopes in Figures 2 and 3 were used in order to separate the contribution of the generated Cl_2 of both HOCl and Cl_2O. Using equations (22) and (23), it is possible to calculate the fraction of the HOCl taken up which leads to the formation of Cl_2:

$$Cl_{2\,(HOCl\ contribution)} = Cl_{2\,(HOCl/Cl2O\ mixture)} - Cl_{2(calculated,\ pure\ Cl2O\ uptake)} \quad (22)$$

$$Cl_{2(calculated,\ pure\ Cl2O\ uptake)} = Cl_2O_{(HOCl/Cl2O\ mixture)} \times S_{(pure\ Cl2O\ uptake)} \quad (23)$$

where $Cl_{2\,(HOCl/Cl2O\ mixture)}$ is the Cl_2 yield generated from simultaneous uptake of both Cl_2O and HOCl, $Cl_{2\,(calculated,\ pure\ Cl2O\ uptake)}$ is the Cl_2 yield generated

according to reactions (18) and (19) and calculated using the corresponding slopes $S_{(pure\ Cl2O\ uptake)}$ from Figure 2. In order to determine the fraction of HOCl that results in Cl_2, $Cl_{2\ (HOCl\ contribution)}$ calculated from equation (22) is plotted as a function of HOCl taken up as shown in Figure 4. The slopes in Figure 4a and 4b are 0.30±0.10 on frozen KCl, NaCl and recrystallized sea salt (RSS), and 0.23±0.13 on frozen NSS solution, respectively, at 200 K. Given the scatter in the results displayed in Figure 4b, we conclude that between 10 and 40% of the HOCl taken up is converted to Cl_2 on both frozen KCl and NSS solution at 200 K, independent of the frozen substrate and after correction for the formation of Cl_2 from Cl_2O following equations (22) and (23).

In conclusion the data displayed in Figure 2 reveal that the Cl_2 yield per Cl_2O taken up is 2.8 times higher for NSS than for the remainder of the substrates for pure Cl_2O, that is without interference from HOCl. Figure 3 reveals that for the $Cl_2O/HOCl$ mixture the Cl_2 yield per Cl_2O taken up is significantly higher on all Cl-containing substrates compared to pure Cl_2O. It is suggested that this yield increase, expressed as an average slope of 1.46 in Figure 3 compared to 1.11 in Figure 2 is due to the presence of HOCl in the reacting gas. Figure 4 finally displays a fairly weak Cl_2 yield of 0.3±0.1 per HOCl taken up, regardless of the substrate and after correction for the Cl_2 yield caused by Cl_2O. We propose to use the slopes as a parameter describing the relative propensity of Cl_2O and HOCl to generate Cl_2 from chloride-containing substrates at 200 K. It thus turns out that Cl_2O generates roughly twice the Cl_2 yield compared to HOCl taking the ratio of slopes of 1.11 vs. 0.3 and normalizing the yield per Cl atom capble of generating Cl_2. In addition, Table 5 reveals that a large fraction of HOCl may be recovered through desorption at 240 K in contrast to Cl_2O that has all but disappeared. In summary, the quantitative results show that the Cl_2 yields per HOCl taken up are significantly lower than for pure Cl_2O taken up on both frozen KCl, NaCl, RSS and NSS solutions thus reflecting the lower reactivity of HOCl compared to Cl_2O for uptake on frozen halide solutions. This remains valid even when taking into account the redox properties of humic-like substances that may occur in NSS [33,34].

4. Br_2 single pulse event

Immediately after the exposure of the $HOCl/Cl_2O$ mixture or pure Cl_2O on the frozen NSS solution for concentrations larger than 10^{11} molecule cm^{-3}, a single Br_2 pulse event of approximately $(1.0\pm0.3)\times10^{15}$ molecules occurs during the first moments of the experiment. Br_2 pulse events are displayed in Figures 5a and 5b for pure Cl_2O and $HOCl/Cl_2O$ uptake on NSS frozen solution, respectively. By performing repetitive uptake experiment on frozen NSS solution, we do not detect additional Br_2 bursts. We thought at first that only the surface adsorbed Br^- were consumed in the first Cl_2O or HOCl uptake. However, no additional Br_2 bursts could be observed once the exposed sample had melted and

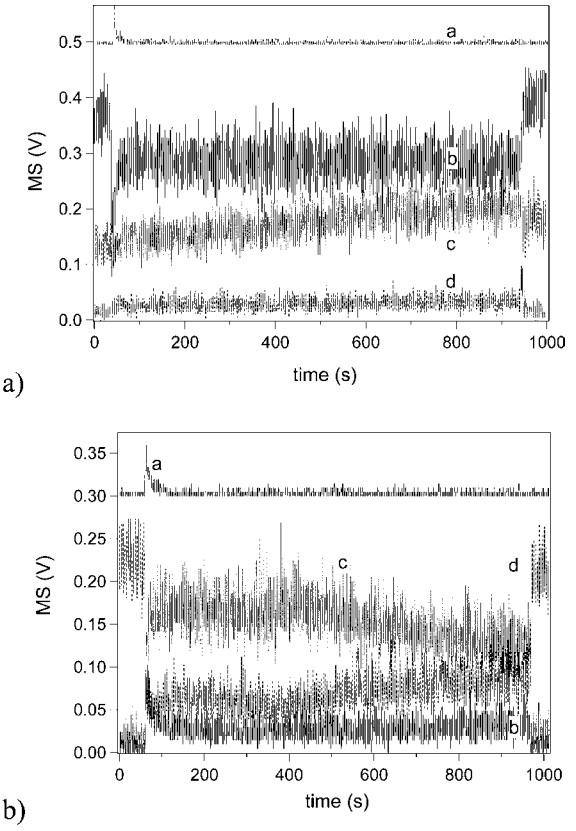

Fig. 5. Uptake of pure Cl_2O (a) and $HOCl/Cl_2O$ mixture (b) on frozen NSS solution at 200 K for an escape orifice of 4 mm diameter. The symbols a, b, c and d correspond to the MS signal of Br_2 (m/e 160), HOCl (m/e 52), Cl_2 (m/e 70) and Cl_2O (m/e 51), respectively.

let above 273 K for 20 minutes before freezing the sample and performing a second HOCl or Cl_2O uptake. This may be related to the slow rate of diffusional mixing at temperatures in the vicinity of 273 K which prevents the effective replacement of a Br-depleted solution from the interface by fresh bulk.

One in 600 of NaCl is Br^- in NSS solution resulting in approximately 0.001 M of Br^-. This represents approximately 6×10^{20} Br^- per dm^3 of solution. In the present experiments, 5 ml of solution containing 35 gl^{-1} of NSS was poured into the sample holder and resulted in $V_{frozen} = V_{sol}$ $(\rho_{frozen}/\rho_{sol})$ = 4.5 cm^3, where V_{sol} = 5 cm^3 is the volume of the liquid solution, ρ_{sol} = 1.02 g cm^{-3} and ρ_{frozen} = 0.92 g cm^{-3} are the densities of the liquid and of the frozen solution, respectively. This amounts to 3×10^{18} Br^- cm^{-3} and reveals that $2\times10^{15}/2.7\times10^{18}$ = 0.08% of the total Br^- in the sample was available to

react and produce Br_2 on frozen NSS solution at 200 K for both Cl_2O and HOCl/Cl_2O uptake.

It was found in previous work [35] that HOBr taken up on frozen chloride solution is completely converted to BrCl rather than transformed to Br_2. In contrast, HOCl taken up on frozen bromide solution mostly produces Br_2. In conclusion, even if only 0.08% Br^- is activated in the atmosphere, it could have significant implication on the composition of the marine boundary layer because only catalytic amounts of Br_2 are necessary to start polar sunrise chemistry.

5. Influence of concentration, residence time and temperature on the Cl_2 yield

Switching from the 4 to 14 mm diameter escape aperture reduces both the residence time as well as the pressure in the reactor by a factor of 12 according to Table 1. Under those conditions the chlorine mass balance for uptake of both pure Cl_2O and HOCl/Cl_2O at T = 200 K is not satisfied anymore as may be seen from Table 6 because 20 to 30% of the dosed chlorine is not recoverable by thermal desorption at 240 K. The quantity of dissolved Cl_2O and/or HOCl is probably too small for it to desorb at 240 K

Figure 6b displays the yield of Cl_2 resulting from pure Cl_2O uptake on frozen KCl solution at 200 K as a function of time as well as of Cl_2O taken up for a single uptake experiment. A slope of 1.0 means that 50% of the chlorine taken up as Cl_2O turns up as Cl_2. We note that the scale of the exposure time is not necessary linear with the uptake of Cl_2O as it depends on the temporal dependence of the uptake. The data in Figure 6b are to be compared with Figure 7b corresponding to HOCl/Cl_2O uptake on frozen KCl solution at 200 K. Comparison of the slopes in Figures 6b and 7b at steady state (for $t > 350$ s) leads to the conclusion that they are identical within experimental uncertainty. The same is true for HOCl/Cl_2O and Cl_2O uptake on frozen NSS solution at 200 K whose data are not shown. This together with a comparison of the cumulative yields of Cl_2 relative to Cl_2O and HOCl in pure Cl_2O and HOCl/Cl_2O uptakes at 200 K, respectively, strongly suggests that the uptake of HOCl by itself does not lead to Cl_2 formation at the low partial pressures used under the assumption that Cl_2O and HOCl uptake are independent of each other. Table 5 hints at the inhibition of Cl_2O uptake in the presence of HOCl as do the data of Table 5, as mentioned above, and suggest that the assumption of complete independence between HOCl and Cl_2O may not hold. Consequently, HOCl is reactive only on frozen salt solutions for concentrations on the order of 10^{11} HOCl cm^{-3} corresponding to 10 ppb or more. This in turn suggests that the species taken up is in reality Cl_2O whose formation from HOCl is favored at high [HOCl].

Uptake experiments of pure Cl_2O and HOCl/Cl_2O at 215 K obtained in the 4 mm diameter aperture reactor revealed the same results as for the 14 mm diameter orifice reactor discussed above, namely that there is no additional for-

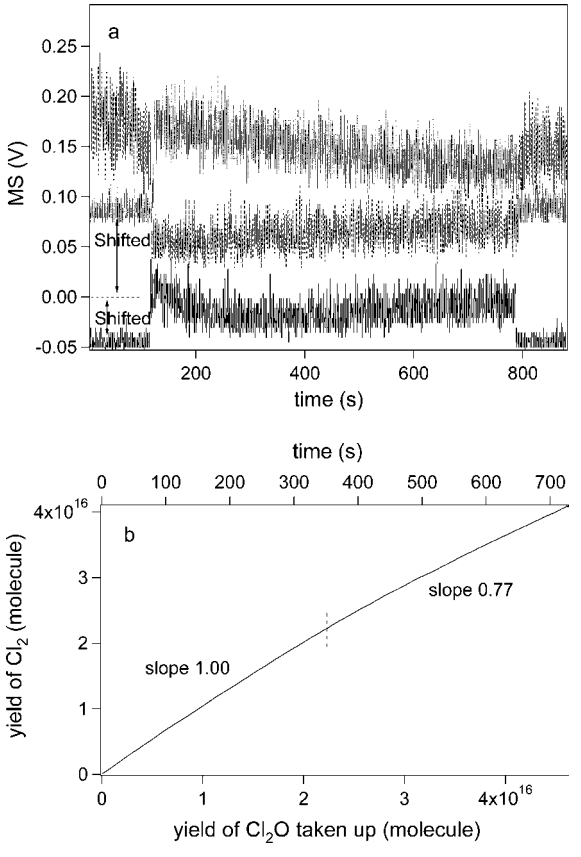

Fig. 6. (a) and (b): pure Cl_2O uptake on frozen KCl solution at 200 K for $[Cl_2O] = 1.9 \times 10^{10}$ molecule cm^{-3} using an escape orifice of 14 mm diameter. (b) Cl_2 yield as a function of Cl_2O taken up for raw data displayed in (a). On graph (a), the dotted and solid curves show the formation of Cl_2 and HOCl, respectively. The hashed curve corresponds to uptake of Cl_2O.

mation of Cl_2 due to heterogeneous interaction of HOCl with frozen salt solutions beyond the one generated by the reaction of Cl_2O. Moreover, the Cl_2O heterogeneous reaction is again significantly inhibited by the presence of HOCl. Comparison of the Cl_2 yields with Cl_2O and HOCl uptake at 215 K/4 mm diameter orifice reactor listed in Table 6 confirms both results, namely absence of Cl_2 formation from HOCl alone, and strong inhibition of Cl_2O uptake in the presence of HOCl. Figures 13 and 14 present time-dependent cumulative yields of Cl_2 also as a function of Cl_2O uptake, and confirm the above conclusions. It therefore seems that Cl_2O is more reactive than HOCl on frozen salt solutions at 200 and 215 K as far as Cl_2 release is concerned. In addition, the slightly larger slopes in going from Figures 13a and 14a indicate that the Cl_2 yields per Cl_2O taken up increase with temperature in the range 200 to 215 K.

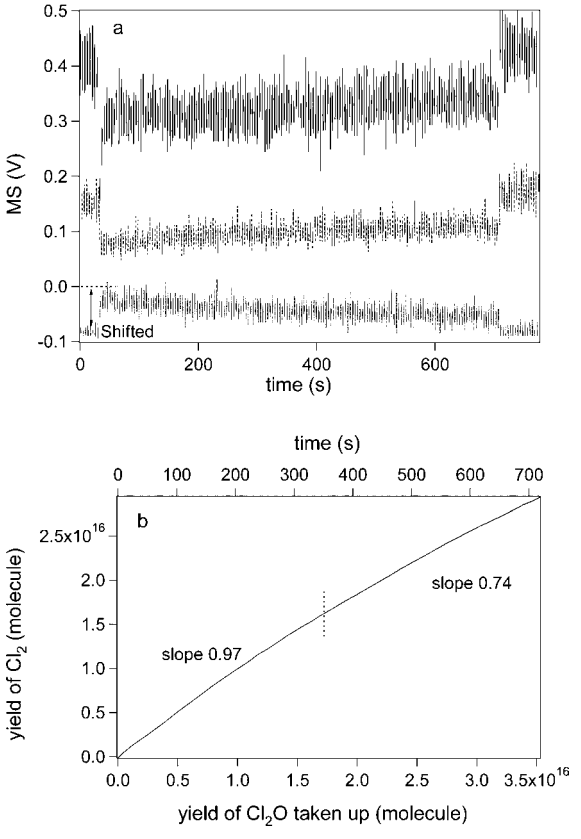

Fig. 7. (a) and (b). $HOCl/Cl_2O$ uptake on frozen KCl solution at 200 K for [HOCl] = 3.7×10^{10} molecule cm^{-3} using an escape orifice of 14 mm diameter. (b) Cl_2 yield as a function of Cl_2O taken up and exposure time t for raw data displayed in (a). On graph (a), the dotted and solid curves show the formation of Cl_2 and the uptake of HOCl, respectively. The dashed curve corresponds to uptake of Cl_2O.

6. Uptake coefficient of Cl_2O and HOCl

The uptake kinetics for fresh frozen KCl solutions at 200 K are displayed in Table 2 and Figure 8 in terms of γ_{ss}(HOCl) which increases by a factor of ten when [HOCl] decreases from 10^{11} to 10^{10} molecule cm^{-3} (see Table 1). Uptake coefficients were obtained by averaging over at least two uptake experiments. We also note that $\gamma_{ss}(Cl_2O)$ for the mixture $HOCl/Cl_2O$ is less than 10^{-3} for [HOCl] > 10^{11} molecule cm^{-3}, but is larger than 0.1 for [HOCl] < 10^{11} molecule cm^{-3}. This inhibition effect was briefly discussed above in relation to the total uptakes and may occur owing to high surface concentrations of both HOCl

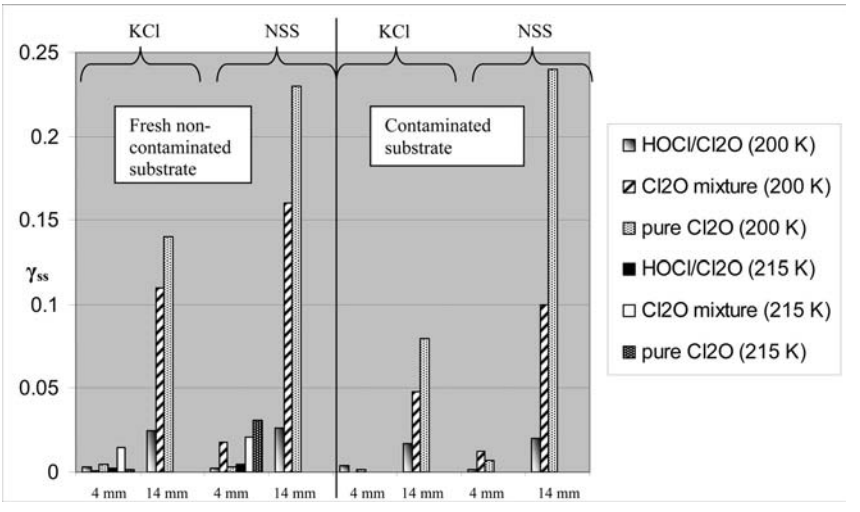

Fig. 8. Synopsis of steady state uptake coefficients γ_{ss} for HOCl and Cl_2O on frozen salt solutions of KCl and NSS at different experimental conditions. The uptake coefficient measured corresponds to the species first mentioned in the legend. The uncertainties in γ_{ss} are estimated as ±10 %.

and/or Cl_2O. This may lead to surface site saturation on the time scale of the experiment and reveals complex kinetics at the gas-condensed phase interface.

$\gamma_{ss}(Cl_2O)$ for pure Cl_2O uptake at $[Cl_2O] < 10^{11}$ molecule cm^{-3} is larger than 0.05 on fresh and poisoned frozen KCl solution as displayed in Tables 2 and 3, respectively. In addition, $\gamma_{ss}(Cl_2O)$ for pure Cl_2O on frozen KCl solution for $[Cl_2O]$ between 10^{10} to 10^{12} molecule cm^{-3} decreases by a factor of two for the second uptake. In contrast, $\gamma_{ss}(Cl_2O)$ for pure Cl_2O on frozen NSS solution increases at least by a factor of two for the second uptake for $[Cl_2O] > 10^{11}$ molecule cm^{-3} (4 mm diameter orifice). However, $\gamma_{ss}(HOCl(Cl_2O))$ on frozen NSS solution did not change for concentrations ranging from 10^{10} to 10^{12} molecule cm^{-3} and for a fresh or a previously poisoned sample within the experimental uncertainty as displayed in Tables 3 and 4.

The measured uptake coefficient of Cl_2O for the mixture $HOCl/Cl_2O$, $\gamma_{ss}(Cl_2O(HOCl))$, interacting with frozen NSS solution for [HOCl] ranging from 10^{10} to 10^{12} molecule cm^{-3} was found to be ten times smaller compared to the uptake of pure Cl_2O on the same substrate, that is in the absence of HOCl. This may be explained either by the reverse of reaction (12) when HOCl is admitted into the reactor and more Cl_2O is generated on the ice that may lead to surface saturation, or by the known propensity of HOCl to poison ice surfaces that is in contrast to the adsorption of Cl_2O on pure ice discussed in 3.1.

In summary, the kinetics of repetitive uptake for both Cl_2O and HOCl on a frozen KCl or NSS salt solution will lead to a decrease of γ_{ss}. In contrast, γ_{ss}

increases when the sum of [HOCl] and [Cl_2O] decrease below 10^{11} molecule cm^{-3}. In addition, γ_{ss} is generally larger on frozen NSS compared to KCl salt solution for a given HOCl and Cl_2O concentration at 200 or 215 K (see Tables 3, 4 and 5 and Figure 8). Figure 8 conveys an impression on the relative magnitude of γ_{ss} of HOCl vs. Cl_2O and underlines the fact that Cl_2O uptake is significantly faster under all conditions. Previous work [31] has investigated the HOCl uptake on frozen KCl ice film of 0.1% by weight at 233 K which resulted in $\gamma_{ss}(HOCl) < 4.7 \times 10^{-2}$. In the present work, we have used a concentration of 35 g l^{-1} of KCl which corresponds to approximately 0.2% by weight of Cl^-. For a frozen KCl and NSS salt solution at 215 K we have obtained $\gamma_{ss}(HOCl) = (2.1 \pm 0.6) \times 10^{-3}$ and $\gamma_{ss}(Cl_2O) = (4.6 \pm 1.4) \times 10^{-3}$, respectively. These values are consistent with the results presented by Huff and Abbatt at 233 K [35].

7. Atmospheric implications and conclusions

We conclude that significant differences in the yield of Cl_2 owing to Cl_2O uptake were observed depending on the nature of the frozen substrate. For this reason KCl and NaCl may not in general be used as a model for NSS that shows special properties in comparison with the other three chloride-containing substrates, namely KCl, NaCl and RSS frozen solution. The reason for this special behaviour may lie either in the buffering capacity or the presence of oxidizable organic substances, as alluded to above.

HOCl is thermodynamically unstable and is in equilibrium with Cl_2O according to reaction (12) and its inverse. The standard heat of reaction of equilibrium (12), ΔH_r^0, has been measured by several authors, but we prefer the value of Knauth et al. [23] owing to the quality of this study with $\Delta H_r^0 = 2.7 \pm 0.2$ kcal/Mol leading to $K^{298} = 0.082$ (dimensionless). The kinetic results of this work including the comparison of the reactivity of pure Cl_2O and a (non-equilibrium) mixture of HOCl/Cl_2O which we are able to prepare with routinely 25% Cl_2O in the HOCl sample (see Experimental) suggest that the equilibrium (12) lies on the side of adsorbed HOCl in the presence of ice or frozen aqueous salt solutions according to equilibrium (24):

$$Cl_2O(ads) + H_2O(ice) \rightleftharpoons 2\ HOCl(ads) \qquad (24)$$

The present results are consistent with a parallel reaction scheme in which Cl_2O directly reacts with Cl^- to Cl_2, either through halogen exchange, reaction (19), or through a redox reaction on NSS as mentioned above. Unreacted Cl_2O may form HOCl(ads) that is non-reactive by itself but that slowly may react on the ice surface by way of equilibrium (24) and regenerate reactive Cl_2O. Therefore, equilibrium (24) is essential in considering the heterogeneous halogen forming potential of HOCl in the troposphere at suitably low temperatures. The possible reason for the exothermicity of equilibrium (24) in the forward direction, which is in contrast to the gas phase, may lie in the ability of HOCl to form

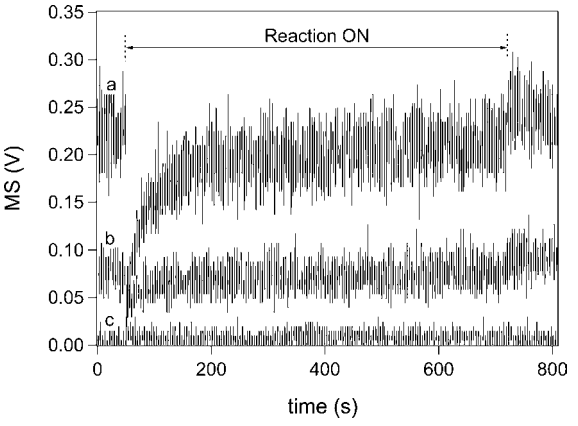

Fig. 9. HOCl uptake on pure bulk (B) ice held at 200 K using the 4 mm diameter escape aperture. Curves a (HOCl), b (Cl_2O) and c (Cl_2) were monitored at m/e = 52, 51 and 70, respectively. The HOCl and Cl_2O flow rates correspond to $(5.0\pm1.5)\times10^{14}$ and $(1.1\pm0.5)\times10^{14}$ molecule s^{-1}, respectively. The corresponding concentrations of HOCl and Cl_2O were 4.5×10^{11} and 1.5×10^{11} molecule cm^{-3}, respectively.

strong hydrogen bonds with the ice surface, a property that Cl_2O lacks. Although we do not observe Cl_2 formation by HOCl itself at low residence times (14 mm diameter orifice) or at higher temperature of 215 K in the present experiments we cannot discount the possibility that Cl_2 may form at atmospherically meaningful time scales such as days if we allow the ice substrate to accumulate sufficient HOCl such that reactive Cl_2O may be generated following equilibrium (24). Formation of Cl_2 is subsequently expected in view of the high reactivity of Cl_2O(ads) observed in the present study. We therefore postulate that there is a role for HOCl in regards to formation of Cl_2 in marine boundary layer chemistry at low temperatures although there is no experimental proof available from gas phase measurements yet.

There have been a number of theoretical studies on the interaction of HOCl with ice surfaces, but none with Cl_2O such that the quantitative aspects of equilibrium (24) remain to be elucidated [36–38]. However, the present results offer a glimpse on the qualitative behaviour of adsorbed HOCl/Cl_2O by using the Cl_2 formation as a probe. The present results are also broadly consistent with Huff and Abbatt [25] who conducted the only other study with which the present work is comparable. They noted that HOCl is nonreactive on ice substrates at 233 and 248 K and provided upper limits for γ_{ss} that are consistent with the present values.

In an atmospheric context, we may estimate the yield of Cl_2 from the uptake of HOCl on marine ices using the present experimental results. From the work of Huff et Abbatt [25], it is possible to estimate the flux of the dry deposition of HOCl using F = v C, where v is the vertical deposition velocity in cm s^{-1} and

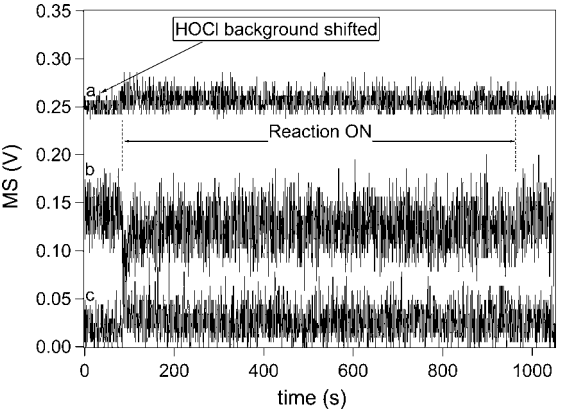

Fig. 10. Cl_2O uptake on pure bulk (B) ice held at 200 K using the 4mm diameter escape aperture. Curves a (HOCl), b (Cl_2O) and c (Cl_2) were monitored at m/e = 52, 51 and 70, respectively. The Cl_2O impurity flow rate was $(2.4\pm0.6)\times10^{14}$ molecule s^{-1}.

C is the HOCl concentration in the atmosphere in molecule cm^{-3}. Results from field measurements revealed that the concentration of chloride compounds that could be photolysed (HOCl or Cl_2) is approximately 10 ppt [7] which corresponds to 2.95×10^8 HOCl cm^{-3} in the spring time. The vertical velocity of the dry deposition is calculated using $v = 1/(R_a + R_b + R_c)$, where R_a is the transport of HOCl across the atmospheric boundary layer, R_b is the molecular diffusion term and R_c is the contribution of the heterogeneous reaction expressed in s cm^{-1}. $R_a = (1/uk^2)(\ln(z/z_0))^2$, where u is the wind velocity taken as 1000 cm s^{-1}, k is a proportionality factor equal to 0.4, $z_0 = 10^{-5}$ m is the length of the ice roughness and z is the height of an atmospheric layer taken to be 100 m [39]. In addition, $R_b = z_0/D(HOCl)$ where $D(HOCl) = 0.105$ cm^2 s^{-1} is the HOCl diffusion coefficient in air. Finally, $R_c = 4/\gamma c$ where c is the mean molecular velocity of HOCl. Using as an estimate $\gamma_{ss}(HOCl) \approx 2\times10^{-3}$ on frozen NSS solution at 200 K for [HOCl] $>10^{11}$ molecule cm^{-3} (see Table 2), we obtain v(HOCl) = 0.589 cm s^{-1} which leads to F(HOCl) = (2.95×10^8 molecule cm^{-3}) (0.589 cm s^{-1}) = 1.74×10^8 molecule cm^{-2} s^{-1}. Under the assumption that 30% of HOCl taken up on marine ice is converted to Cl_2 at 200 K, we estimate that $F(Cl_2) = (1.74\times10^8$ molecule cm^{-2} $s^{-1})$ (0.30) = 5.22×10^7 molecule cm^{-2} s^{-1} at 200 K.

By considering the formation of Cl_2 as an upper limit from the reaction of HOCl on marine ice for half a day, we obtain (5.22×10^7 molecule cm^{-2} s^{-1})(43200 s) = 2.25×10^{12} molecule of Cl_2 produced per cm^2 of marine ice per day. If Cl_2 is mixed homogeneously in the atmosphere within a layer of 100 m, the Cl_2 concentration could reach up to 2.25×10^8 molecule cm^{-3} or 9 ppt. This order of magnitude estimate may confirm that halogen

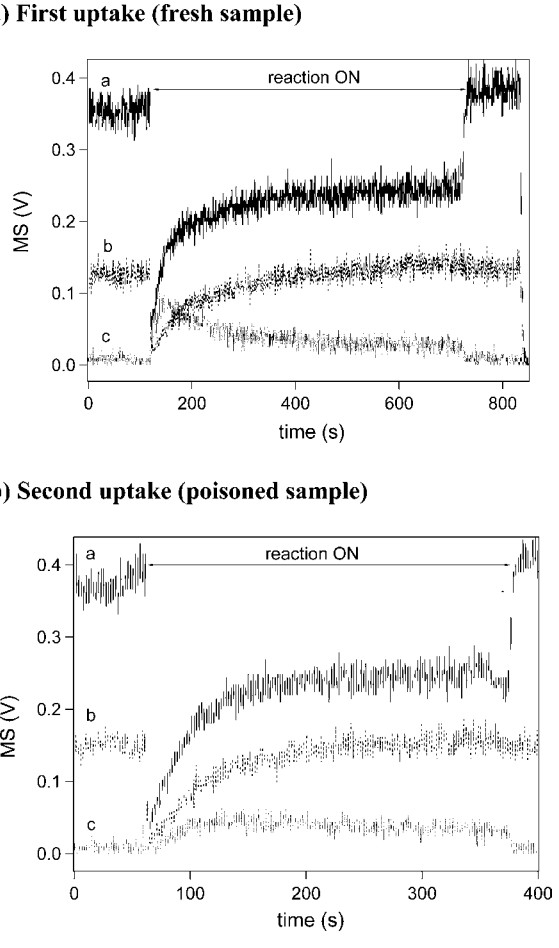

Fig. 11. Repetitive HOCl uptake on frozen KCl solution at 200 K. The HOCl and Cl_2O flow rate were 8×10^{14} and 2×10^{14} molecule s^{-1}, respectively. The traces a, b and c are related to HOCl (m/e 52), Cl_2O (m/e 51) and Cl_2 (m/e 70) MS signal, respectively at 200 K, 4 mm diameter orifice.

activation effectively could lead to an important destruction of hydrocarbons and ozone in the marine boundary layer during arctic spring time.

The conclusions from the present work may be summarized as follows:

From the comparison of the interaction of pure Cl_2O on the one hand, and of a non-equilibrium mixture of HOCl/Cl_2O on several types of chlorine-containing substrates in the range 200 to 215 K we obtain the indication that the reactivity of Cl_2O is significantly larger than that of HOCl in regards to the formation of Cl_2. As an example, the Cl_2 yield resulting from the interaction of Cl_2O on a frozen salt solution at 200 K is twice that of HOCl.

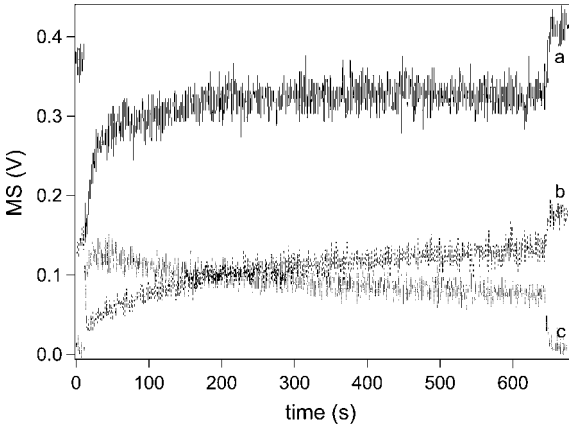

Fig. 12. HOCl uptake on frozen acidified KCl solution at 200 K. The HOCl (a) and Cl_2O (b) flow rate were 9×10^{14} and 2.4×10^{14} molecule s^{-1}, respectively, and led to Cl_2 (c) production. The frozen KCl solution was buffered with 0.068 M NaOH, 0.056 M citric acid and 0.044 M NaCl (pH = 4.0) at 200 K, 4 mm diameter orifice.

Excellent chlorine mass balances are obtained under certain conditions at 200 K, but not at low residence times and/or low pressures as well as at 215 K.

Uptake of both Cl_2O and HOCl on frozen NSS (natural sea salt) solution is sustained for at least an hour in contrast to other chlorine-containing substrates such as frozen KCl, NaCl and RSS (recrystallized sea salt) solution. The facile reactive uptake of HOCl and Cl_2O on NSS may be due to the natural buffering capacity or the presence of oxidizable organics in NSS that both are thought to support the formation of Cl_2.

Cl_2O and/or HOCl uptake on NSS leads to a one-time Br_2 release in a burst mode that may be significant in relation to marine boundary layer chemistry in the springtime arctic.

Owing to the thermodynamic instability of HOCl in the gas phase the fate/formation of the corresponding thermodynamically stable anhydride, Cl_2O, must also be considered in the presence of a substrate with which both species interact. Considering the equilibrium between adsorbed HOCl and Cl_2O on ice it is likely that the gateway to formation of Cl_2 passes through the formation of adsorbed, reactive Cl_2O by way of adsorption of gas phase HOCl on the surface of the frozen aqueous halide.

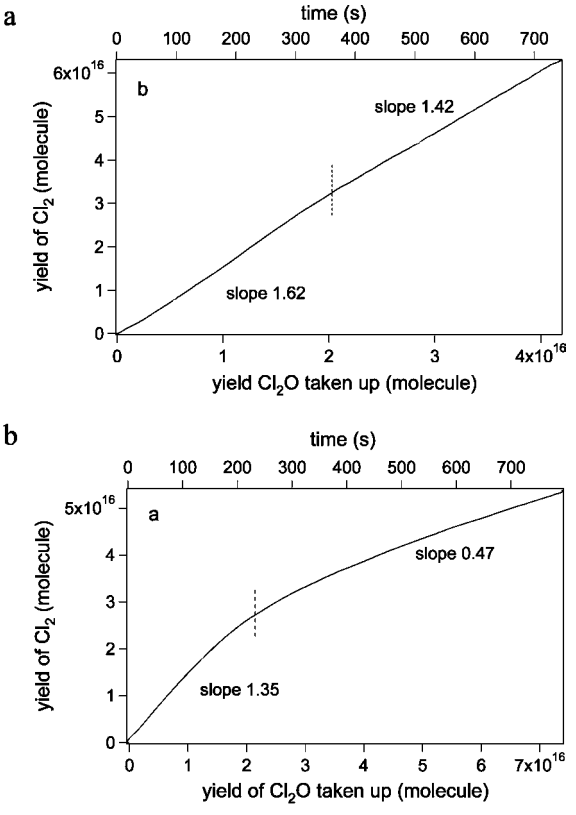

Fig. 13. Uptake of pure Cl_2O (a) and $HOCl/Cl_2O$ (b) on frozen KCl solution at 200 K for [HOCl] = 4.5×10^{11} molecule cm^{-3} (4 mm diameter escape orifice). The Cl_2 yield is plotted as a function of exposure time and Cl_2O taken up.

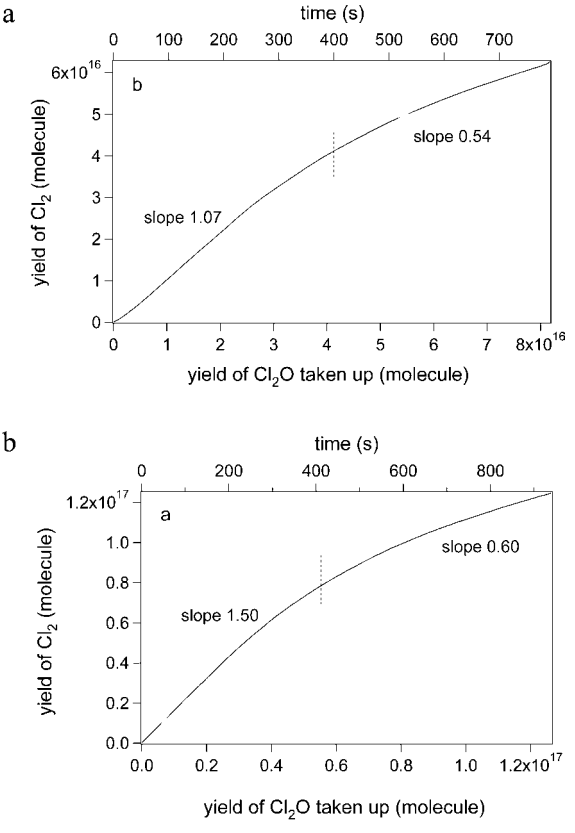

Fig. 14. Uptake of pure Cl_2O (a) and $HOCl/Cl_2O$ (b) on frozen KCl solution at 215 K for [HOCl] = 4.5×10^{11} molecule cm^{-3} (4 mm diameter escape orifice). The Cl_2 yield is plotted as a function of exposure time and Cl_2O taken up.

Appendix

Table 5. Summary of mass balance for uptake experiments of $HOCl/Cl_2O$ and pure Cl_2O on frozen KCl and Natural Sea Salt (NSS) solutions at 200 K at concentrations in excess of 10^{11} molecule cm^{-3} (4 mm diameter escape orifice)[a]. Integration time is 700±50 s.

Reactants	Escape orifice (mm)	Uptake		Products		Thermal desorption at 240 K of chlorine-containing species		Uptake of chlorine species	Recovery of chlorine species	Relative Cl_2 yield	Ratio desorbed vs.remaining HOCl
		(10^{17} Cl_2O)	(10^{17} HOCl)	(10^{17} Cl_2)	(10^{17} HOCl)	(10^{17} Cl_2O)	(10^{17} HOCl)	(10^{17})	(10^{17})		
Cl_2O/KCl (200 K)	4	0.73	0	0.49	0.84	0.016	0.20	1.47	1.56	0.33	-
HOCl/KCl (200 K)	4	0.27	0.63	0.58	-	0.034	0.49	1.17	1.14	0.50	0.77
Cl_2O/NSS (200 K)	4	1.41	0	1.96	0.097	0.037	0.70	2.82	2.83	0.70	-
HOCl/NSS (200 K)	4	1.12	0.80	2.58	-	0.043	0.63	3.04	3.30	0.85	0.79

[a] Each individual yield measurement has an uncertainty of 5% resulting in a 20% uncertainty in the mass balance.

Table 6. Summary of mass balance for uptake experiments of $HOCl/Cl_2O$ and pure Cl_2O on frozen KCl and Natural Sea Salt (NSS) solutions at different temperatures and gas phase residence times at concentrations in excess of 10^{11} molecule cm^{-3} (4 and 14 mm diameter escape orifice)[a].

Reactants	Escape orifice (mm)	Uptake		Products		Thermal desorption at 240 K of chlorine-containing species		Uptake of chlorine species	Recovery of chlorine species	Relative Cl_2 yield	Ratio desorbed vs.remaining HOCl
		(10^{17} Cl_2O)	(10^{17} HOCl)	(10^{17} Cl_2)	(10^{17} HOCl)	(10^{17} Cl_2O)	(10^{17} HOCl)	(10^{17})	(10^{17})		
Cl_2O/ KCl (215 K)	4	1.20	0	1.19	0.60	0	0	2.40	1.79	0.50	-
HOCl/ KCl (215 K)	4	0.80	1.00	0.62	-	0	0	2.60	0.62	0.24	0
Cl_2O/ NSS (215 K)	4	0.83	0	1.10	0.63	0	0	1.67	1.73	0.66	-
HOCl/ NSS (215 K)	4	0.80	0.92	0.82	-	0	0	2.50	0.82	0.33	0
Cl_2O/ KCl (200 K)	14	0.52	0	0.40	0.39	0	0	1.04	0.79	0.37	-
HOCl/ KCl (200 K)	14	0.17	0.38	0.18	-	0	0	0.72	0.18	0.25	0
Cl_2O/SS (200 K)	14	0.61	0	0.79	0.97	0	0	1.22	0.89	0.65	-
HOCl/SS (200 K)	14	0.24	0.45	0.25	-	0	0	0.93	0.25	0.27	0

[a] Each individual yield measurement has an uncertainty of 5% resulting in a 20% uncertainty in the mass balance.

Acknowledgement

Generous support of this research was granted by OFES (Office Fédéral de l'enseignement et de la science, supplanted by the SER agency (State Secretariat for Education and Research)) within the fifth EU framework program project THALOZ.

References

1. L. A. Barrie, J. W. Bottenheim, R. C. Schnell, P. J. Crutzen, R. A. Rasmussen, Nature **334** (1988) 138.
2. L. Barrie, U. Platt, Tellus Series B-Chemical and Physical Meteorology **49** (1997) 450.

3. A. Richter, F. Wittrock, M. Eisinger, J. P. Burrows, Geophys. Res. Lett **25** (1998) 2683.
4. T. Wagner, U. Platt, Nature **395** (1998) 486.
5. B. T. Jobson, H. Niki, Y. Yokouchi, J. Bottenheim, F. Hopper, R. Leaitch, J. Geophys. Res. **99** (1992) 25355.
6. K. L. Foster, R. A. Plastridge, J. W. Bottenheim, P. Shepson, B. J. Finlayson-Pitts, C. W. Spicer, Science **291** (2001), 471.
7. G. A. Impey, P. B. Shepson, D. R. Hastie, L. A. Barrie, K. G. Anlauf, J. Geophys. Res. **102** (1997) 16005.
8. J. P. D. Abbatt, G. C. G. Waschewsky, J. Phys. Chem. A **102** (1998) 3719.
9. S. Fickert, J. W. Adams, J. N. Crowley, J. Geophys. Res. **104** (1999) 719.
10. J. W. Adams, N. S. Holmes, J. N. Crowley, Atmos. Chem. Phys. **2** (2002) 79.
11. R. Vogt, P. J. Crutzen, R. Sander, Nature **383** (1996) 327.
12. J. C. McConnnell, G. S. Henderson, L. Barrie, J. Bottenheim, H. Niki, C. H. Langford, E. M. J. Templeton, Nature **355** (1992) 150.
13. T. Tang, J. C. McConnell, Geophys. Res. Lett. **23** (1996) 2633.
14. Website of the IUPAC Subcommittee on the Evaluation of Data for Atmospheric Chemistry at URL: http://www.iupac-kinetic.ch.cam.ac.uk/
15. B. A. Michalowski, J. S. Francisco, S. M. Li, L. A. Barrie, J. W. Bottenheim, P. B. Shepson, J. Geophys. Res. **105** (2000) 15131.
16. A. Aguzzi, M. J. Rossi, Phys. Chem. Chem. Phys. **1** (1999) 4337.
17. C. Santschi, M. J. Rossi, Phys. Chem. Chem. Phys. **6** (2004) 3447.
18. B. J. Finlayson-Pitts, J. N. Pitts Jr, *Chemistry of the upper and lower atmosphere*, Academy Press, San Diego (2000).
19. S. Ghosal, J. C. Hemminger, J. Phys. Chem. A **103** (1999) 4777.
20. H. N. Berko, P. C. McCaslin, B. J. Finlayson-Pitts, J. Phys. Chem. **95** (1991) 6951.
21. J.-E. L. Cook, C. A. Ennis, T. J. Leck, J. W. Birks, J. Chem. Phys. **74** (1981) 545.
22. C. A. Ennis, J. W. Birks, J. Phys. Chem. **89** (1985) 186.
23. H. D. Knauth, H. Alberti, H. Clausen, J. Phys. Chem. **83** (1979) 1604.
24. L. T. Molina, M. J. Molina, J. Phys. Chem. **82** (1978) 2410.
25. A. K. Huff, J. P. D. Abbatt, J. Phys. Chem. **104** (2000) 7284.
26. T. von Clarmann, N. Glatthor, U. Grabowski, M. Hpfner, S. Kellmann, A. Linden, Gizaw Mengistu Tsidu, M. Milz, T. Steck, G. P. Stiller, H. Fischer, B. Funke, J. Geophys. Res. **111** (2006) D05311.
27. L. J. Kovalenko, K. W. Jucks, R. J. Salawitch, G. C. Toon, J.-F. Blavier, D. G. Johnson, A. Kleinbhl, N. J. Livesey, J. J. Margitan, H. M. Pickett, M. L. Santee, B. Sen, R. A. Stachnik, J. W. Waters, Geophys. Res. Lett. **34** (2007) L19801.
28. F. F. Fenter, F. Caloz, M. J. Rossi, J. Phys. Chem. **98** (1994) 9801.
29. J. Lyman, R. Fleming, Sears Foundation **93** (1939) 143.
30. F. Caloz, F. F. Fenter, K. D. Tabor, M. J. Rossi, Rev. Sci. Instrum. **68** (1997) 3172.
31. P. Pratte and M. J. Rossi, J. Phys. Chem. A **110** (2006) 3042.
32. E. R. Pounder, *The Physics of Ice*, Pergamon Press, Oxford (1965)
33. C. L. Badger, I. George, P. T. Griffiths, C. F. Braban, R. A. Cox, J. P. D. Abbatt Atmos. Chem. Phys. **5** (2005) 9581.
34. V. Vaida, A. F. Tuck, G. B. Ellison, Phys. Chem. Earth (C). **25** (2000) 195.
35. A. K. Huff, J. P. D. Abbatt, J. Phys. Chem. A **106** (2002) 5279.
36. S. Casassa, C. Pisani, J. Chem. Phys. **116** (2002) 9856.
37. B. A. Flowers, J. S. Francisco, J. Phys. Chem. A **105** (2001) 494.
38. A. F. Voegele, C. S. Tautermann, T. Loerting, K. R. Liedl, J. Phys. Chem. A **106** (2002) 7850.
39. J. H. Seinfeld, S. P. Pandis, *Atmospheric Chemistry and Physics*, John Wiley & Sons (1998)
40. L. A. Barrie, G. Denhartog, J. W. Bottenheim, S. Landsberger, J. Atmos. Chem. **9** (1989) 101.